ELSEVIER

Applied Mathematical Modelling 23 (1999) 899–914

APPLIED MATHEMATICAL MODELLING

www.elsevier.nl/locate/apm

Modelling non-Fourier heat conduction with periodic thermal oscillation using the finite integral transform

Bishri Abdel-Hamid [1]

Mathematics and Computer Science, United Arab Emirates University, P.O. Box 17551, Al-Ain, United Arab Emirates

Received 21 May 1998; received in revised form 16 February 1999; accepted 4 March 1999

Abstract

The non-Fourier heat conduction in a finite medium subjected to a periodic heat flux is modelled using the finite integral transform technique and an analytic solution is obtained. An analogy between thermal oscillation and oscillation of mechanical and electrical systems is drawn. A transition criterion from the non-Fourier heat conduction formulation to the Fourier formulation is obtained and a simple analytical expression of the phase and amplitude of thermal oscillation is derived.

Keywords: Non-Fourier heat conduction; Hyperbolic partial differential equations; Finite integral transforms; Periodic thermal oscillation; Heat diffusion modelling

1. Introduction

The use of heat sources such as lasers and microwaves with extremely short duration or very high frequency has found numerous applications in many different areas of mathematical physics, applied sciences and engineering. In such situations, the classical Fourier's heat conduction theory becomes inaccurate and the non-Fourier effect becomes more reliable in describing the diffusion process and predicting the temperature distribution.

The classical theory of heat conduction is based on the un-physical property that heat propagates at an infinite speed. On such basis, the constitutive equation governing heat flow is given by Fourier's law

$$\boldsymbol{q} = -k\nabla T. \tag{1.1}$$

When this relation is incorporated in the local energy balance equation

$$\nabla \cdot \boldsymbol{q} = -\rho c \frac{\partial T}{\partial t}, \tag{1.2}$$

the classical parabolic heat conduction equation

$$\frac{\partial T}{\partial t} = a\nabla^2 T \tag{1.3}$$

[1] E-mail: bishri@nyx.uaeu.ac.ae

0307-904X/99/$ - see front matter
PII: S 0 3 0 7 - 9 0 4 X (9 9) 0 0 0 1 7 - 7

results, provided that k, c and ρ are constant for the given temperature range. In the above equations k is the thermal conductivity of the media, c the specific heat capacity, ρ the mass density and $a = k/\rho c$ the thermal diffusivity. Fourier's law is quite accurate for most common engineering situations. However, for situations involving very short times, temperature near absolute zero or extreme thermal gradients, Fourier's law becomes invalid.

Experimental evidence showed that thermal disturbances appear to propagate as waves at finite speeds in the case of temperature near absolute zero; for instance, in NaF at about 10°K [1], in Bi at 3.4°K [2] and for substances with an extremely ordered internal structure [3]. Recently there has been experimental verification of hyperbolic heat transfer in non-homogeneous materials, such as sand and $NaHCO_3$ which have a relaxation time of about 20 s [4], in super-cooled materials [5] and in biological materials [6]. The non-homogeneous structures apparently induce waves by delaying the response between heat flux and temperature gradient. The delay may represent the time needed to accumulate energy for significant heat transfer between structural elements [4]. The classical Fourier's law does not lead to this type of thermal wave behavior since the law permits the heat flux to respond immediately to changes in temperature gradient.

A modified non-Fourier heat flux equation has been developed by several different approaches [7–14]. When heat waves are important Fourier's conduction law, which connects the heat flux $\boldsymbol{q}$ to the temperature, must be modified by adding an extra thermal inertia term. Vernotte [15] and Cattaneo [16] independently proposed a different constitutive equation for conduction heat transfer in the form

$$\tau \frac{\partial \boldsymbol{q}}{\partial t} + \boldsymbol{q} = -k\nabla T, \tag{1.4}$$

where τ is the relaxation time. The relaxation time depends on the mechanism of heat transport, and represents the time lag needed to establish steady-state heat conduction in an element of volume when a temperature gradient is suddenly applied to that element. An analysis of the compatibility of Eq. (1.4) with the hypothesis of local thermodynamic equilibrium is presented in Ref. [13].

When Eq. (1.4) is used in conjunction with the local energy balance Eq. (1.2), a general hyperbolic equation governing the non-Fourier heat conduction results and can be written in the form

$$a\nabla^2 T = \frac{\partial T}{\partial t} + \tau \frac{\partial^2 T}{\partial t^2}. \tag{1.5}$$

Eq. (1.5) describes heat propagation with a finite speed $V = (k/c\tau)^{1/2}$ and allows a direct determination of the temperature field. It has also been used in modelling a high velocity heat source moving through a medium [17] and in modelling the propagation of the solid–liquid interface during the rapid solidification of liquid metals [18], where convective effects were accounted for in the boundary conditions. It is important, however, to note that non-Fourier conduction is usually associated with micro-scale applications involving very small time and length scales, such as in heating of silicon thin film during integrating circuit fabrication. Convection may not be important in micro-scale applications because of insufficient time for development of fluid motion [19].

The heat flux vector $\boldsymbol{q}$ can be determined by integrating Eq. (1.4) with respect to time to get

$$\boldsymbol{q}(\boldsymbol{x}, t) = \mathrm{e}^{-(t-t_0)/\tau}\boldsymbol{q}(\boldsymbol{x}, t_0) - k/\tau \int_{t_0}^{t} \mathrm{e}^{-(t'-t)/\tau}\nabla T(\boldsymbol{x}, t')\,\mathrm{d}t'. \tag{1.6}$$

Various solutions of the hyperbolic heat conduction equation for finite and semi-infinite media under different boundary conditions can be found in the literature. A semi-infinite medium is considered and a temperature distribution is obtained in Refs. [20–22] due to a step change in temperature at the boundary, in Ref. [23] due to a step change of heat flux, in Ref. [24] due to distributed volumetric energy sources, in Ref. [25] due to internal Joule heating and convection heat exchange with the surrounding and in Ref. [19] due to only surface convection.

The hyperbolic heat conduction in a finite medium has been investigated in Ref. [10] due to a step change of temperature on both sides and in Ref. [26] due to a step change of temperature on one side. A finite slab with volumetric energy source and insulated boundaries is treated in Ref. [27] and a finite slab subject to rectangular heat pulses at one of its surfaces is studied in Ref. [12]. A finite medium with surface radiation boundary condition is considered in Ref. [28] and a finite medium with temperature-dependent conductivity is considered in Ref. [29]. A finite slab exposed to a boundary condition of an instantaneous pulsed heat flux and extended heat flux is reported in Ref. [30]. A very thin solid plate subjected to an asymmetrical temperature change on both surfaces is modelled in Ref. [31].

Most previous works were performed for a pulsed heat flux or for a sudden temperature change. However, for a periodic flux in a finite medium, the work is seldom found in the literature. Recently, a finite medium exposed to a periodic flux was considered in Refs. [32,33], where an analytic solution was derived; however, an analytic expression for the amplitude and phase was not obtainable from that solution.

In this work, we model the hyperbolic heat conduction in a finite medium subjected to a periodic heat source using the finite integral transform technique to obtain, in a straightforward manner, a different form of the analytic solution compared to that obtained in Ref. [33]. Analytic expressions for the amplitude and phase are obtained and an analogy between thermal oscillation and mechanical oscillation is presented. The present work complements the author's previous work on parabolic partial differential equations under periodic boundary condition [34,35].

2. Mathematical analysis

The present investigation concerns a finite medium with insulated boundaries where one-dimensional heat conduction and constant thermal properties are considered to prevail. The medium of thickness ℓ is assumed initially in equilibrium at temperature $T(x,0)=0$. At time $t=0$ the external surface at $x=0$ is exposed to a periodic heat flux with amplitude q_0 and frequency ω. The situation is illustrated schematically in Fig. 1.

2.1. Governing equations

The propagation of thermal energy for this physical problem is described by the one-dimensional form of Eq. (1.5), namely

$$a\frac{\partial^2 T}{\partial x^2}=\frac{\partial T}{\partial t}+\tau\frac{\partial^2 T}{\partial t^2}. \tag{2.1}$$

This hyperbolic heat equation is now considered subject to the following boundary and initial conditions

$$-k\frac{\partial}{\partial x}T(0,t)=\tau\frac{\partial}{\partial t}q(0,t)+q(0,t),\quad \frac{\partial}{\partial x}T(\ell,t)=0, \tag{2.2}$$

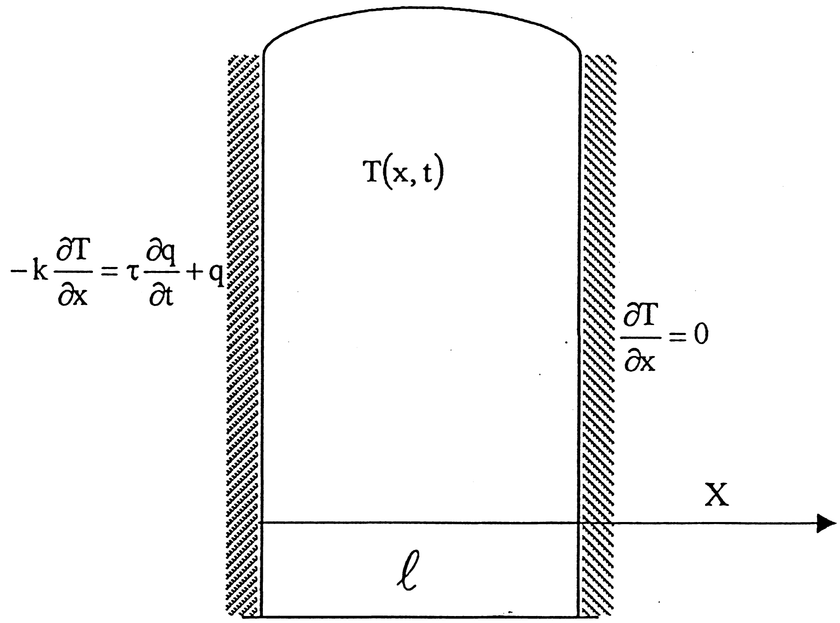

Fig. 1. A schematic representation of geometry and coordinates.

$$T(x,0) = 0, \quad \frac{\partial}{\partial t} T(x,0) = 0, \tag{2.3}$$

where $q(0,t) = q_0 \cos \omega t$ and $q(x,0) = 0$.

Introducing the following dimensionless parameters

$$\eta = \frac{x}{\ell}, \quad \zeta = \frac{at}{\ell^2}, \quad v = \frac{\sqrt{a\tau}}{\ell}, \quad \mu = \frac{a}{\omega \ell^2}, \quad U(\eta,\zeta) = \frac{T(\eta,\zeta)}{q_0/\rho c \omega \ell} \tag{2.4}$$

into Eqs. (2.1)–(2.3), we obtain the non-dimensional form of the non-Fourier heat conduction equation as

$$\frac{\partial^2 U}{\partial \eta^2} = \frac{\partial U}{\partial \zeta} + v^2 \frac{\partial^2 U}{\partial \zeta^2}, \tag{2.5}$$

$$-\frac{\partial}{\partial \eta} U(0,\zeta) = \frac{1}{q_0 \mu}\left[v^2 \frac{\partial}{\partial \zeta} q(0,\zeta) + q(0,\zeta)\right], \quad \frac{\partial}{\partial \eta} U(1,\zeta) = 0, \tag{2.6}$$

$$U(\eta,0) = 0, \quad \frac{\partial}{\partial \zeta} U(\eta,0) = 0, \tag{2.7}$$

with

$$q(0,\zeta) = q_0 \cos \frac{\zeta}{\mu}, \quad q(\eta,0) = 0. \tag{2.8}$$

In the above equations ζ is the Fourier number, v the Vernotte number (also known as the relaxation Fourier number) and is related to the propagation speed, V, of temperature wave by $V = 1/v$.

2.2. Developing the transformation pair

The analytical solution of the above system is obtained by the application of the finite integral transform technique. The procedure is initiated by considering the homogeneous problem associated with the original problem given by Eqs. (2.5)–(2.7), namely,

$$U_{\eta\eta} = U_{\zeta} + v^2 U_{\zeta\zeta}, \tag{2.9}$$

$$U_{\eta}(0,\zeta) = U_{\eta}(1,\zeta) = U(\eta,0) = U_{\zeta}(\eta,0) = 0. \tag{2.10}$$

Separation of variables in Eqs. (2.9) and (2.10) leads to the following eigenvalue problem

$$\Phi''(\eta) + \lambda_n^2 \Phi(\eta) = 0, \tag{2.11}$$

$$\Phi'(0) = \Phi'(1) = 0, \tag{2.12}$$

for which the eigenfunctions and eigenvalues are given by

$$\Phi_n(\eta) = \cos(\lambda_n \eta), \quad \lambda_n = n\pi, \ \ n = 0, 1, 2, \ldots \tag{2.13}$$

The eigenfunctions form an orthogonal set in terms of which we can express the solution of the original problem as

$$U(\eta,\zeta) = \sum_{n=0}^{\infty} c_n(\zeta)\Phi_n(\eta). \tag{2.14}$$

Operating on both sides by $\int_0^1 \Phi_n(\eta)\,\mathrm{d}\eta$ and utilizing the orthogonality relation [36], yields

$$c_n(\zeta) = \frac{1}{N(\lambda_n)} \int_0^1 U(\eta,\zeta)\Phi_n(\eta)\,\mathrm{d}\eta,$$

and Eq. (2.14) becomes

$$U(\eta,\zeta) = \sum_{n=0}^{\infty} \frac{\Phi_n(\eta)}{N(\lambda_n)} \int_0^1 U(\eta,\zeta)\Phi_n(\eta)\,\mathrm{d}\eta, \tag{2.15}$$

where,

$$N(\lambda_n) = \int_0^1 \Phi_n^2(\eta)\,\mathrm{d}\eta. \tag{2.16}$$

On defining the integral transform as

$$\overline{U}_n(\zeta) = \int_0^1 U(\eta,\zeta)\Phi_n(\eta)\,\mathrm{d}\eta, \tag{2.17}$$

the inversion formula becomes

$$U(\eta,\zeta) = \sum_{n=0}^{\infty} \frac{\Phi_n(\eta)\overline{U}_n(\zeta)}{N(\lambda_n)}. \tag{2.18}$$

Eqs. (2.17) and (2.18) define the integral transformation pair needed for the solution.

2.3. The transformed problem

We now use the transformation pair to remove the spatial variable and reduce the original hyperbolic partial differential equation into a second order ordinary differential equation in the temporal variable. The process is initiated by operating on Eq. (2.5) by $\int_0^1 \Phi_n(\eta)\,\mathrm{d}\eta$ and utilizing the definition of the integral transform (2.17) to get

$$\int_0^1 \Phi_n(\eta)\frac{\partial^2 U}{\partial\eta^2}\,\mathrm{d}\eta = \frac{\mathrm{d}\overline{U}_n(\zeta)}{\mathrm{d}\zeta} + v^2\frac{\mathrm{d}^2\overline{U}_n(\zeta)}{\mathrm{d}\zeta^2}. \tag{2.19}$$

The left-hand side is integrated by parts twice and the result is simplified by making use of the boundary conditions given in Eqs. (2.6) and (2.12) to obtain,

$$\int_0^1 \Phi_n(\eta)\frac{\partial^2 U}{\partial\eta^2}\,\mathrm{d}\eta = \int_0^1 U(\eta,\zeta)\,\frac{\mathrm{d}^2\Phi_n}{\mathrm{d}\eta^2}\mathrm{d}\eta + \frac{1}{q_0\mu}\left[v^2\frac{\partial}{\partial\zeta}q(0,\zeta) + q(0,\zeta)\right]. \tag{2.20}$$

The integral on the right side of Eq. (2.20) is evaluated by operating on Eq. (2.11) by $\int_0^1 U(\eta,\zeta)\,\mathrm{d}\eta$ and utilizing the definition (2.17). Inserting the result into Eq. (2.19), one obtains

$$\frac{\mathrm{d}^2\overline{U}_n(\zeta)}{\mathrm{d}\zeta^2} + 2P\frac{\mathrm{d}\overline{U}_n(\zeta)}{\mathrm{d}\zeta} + \omega_n^2\overline{U}_n(\zeta) = \frac{1}{q_0\mu}\left[\frac{\partial}{\partial\zeta}q(0,\zeta) + 2Pq(0,\zeta)\right], \tag{2.21}$$

subject to the transformed initial conditions

$$\overline{U}_n(0) = \frac{\mathrm{d}}{\mathrm{d}\zeta}\overline{U}_n(0) = 0, \tag{2.22}$$

where $P = 1/2v^2$ and $\omega_n = \lambda_n/v$. Thus, the hyperbolic problem given by Eqs. (2.5)–(2.7) is reduced to a linear second order ordinary differential equation in only the temporal variable and the boundary conditions of the original problem are incorporated in the non-homogeneous term.

2.4. Solution

The ordinary differential Eq. (2.21) has characteristic roots given by $-P \pm \sqrt{P^2 - \omega_n^2}$ and its general solution consists of a complementary solution $\overline{U}_c(\zeta)$ and a particular solution $\overline{U}_p(\zeta)$. Since $\lambda_n = 0$ is an eigenvalue of the problem given by Eqs. (2.11) and (2.12), we consider the cases when $\lambda_n = 0$, $P > \omega_n$, and $P < \omega_n$. The complementary and particular solutions are evaluated for each of the three cases.

2.4.1. Case 1: Solution for $\lambda_n = 0$

For this case

$$\overline{U}_c^0(\zeta) = A_1 + A_2 e^{-2P\zeta}, \tag{2.23}$$

$$\overline{U}_p^0(\zeta) = \frac{1}{\mu q_0}\int q(0,\zeta)\,\mathrm{d}\zeta. \tag{2.24}$$

The transformed initial conditions (2.22) and the condition imposed on q in Eq. (2.8) yield $A_1 = A_2 = 0$, and Eq. (2.23) gives

$$\overline{U}_0(\zeta) = \sin\frac{\zeta}{\mu}. \tag{2.25}$$

2.4.2. Case 2: Solution for $P > \omega_n$

For this case the complementary solution is

$$\overline{U}^R_{\mathrm{c}}(\zeta) = \mathrm{e}^{-P\zeta}\Big[A_1 \exp\Big(\sqrt{P^2-\omega_n^2}\zeta\Big) + A_2 \exp\Big(-\sqrt{P^2-\omega_n^2}\zeta\Big)\Big], \tag{2.26}$$

the particular solution may be written in the form

$$\overline{U}^R_{\mathrm{p}}(\zeta) = C_n \sin\frac{\zeta}{\mu} + D_n \cos\frac{\zeta}{\mu}, \tag{2.27}$$

and the general solution is

$$\overline{U}^R_n(\zeta) = \overline{U}^R_{\mathrm{c}}(\zeta) + \overline{U}^R_{\mathrm{p}}(\zeta). \tag{2.28}$$

For the given set of initial conditions,

$$A_1 = -\frac{-(P+\beta)\delta_-}{2\beta\big(1+\delta_-^2\big)}, \quad A_2 = \frac{(P-\beta)\delta_+}{2\beta\big(1+\delta_-^2\big)},$$

$$C_n = \frac{(1+\delta_-\delta_+) + \big(\delta_+^2+\delta_-^2\big)}{\big(1+\delta_+^2\big)\big(1+\delta_-^2\big)}, \quad D_n = \frac{\delta_-\delta_+(\delta_+ + \delta_-)}{\big(1+\delta_+^2\big)\big(1+\delta_-^2\big)}, \tag{2.29}$$

with

$$\delta_\pm = \mu(P \pm \beta), \quad \beta = \sqrt{P^2-\omega_n^2}. \tag{2.30}$$

2.4.3. Case 3: Solution for $P < \omega_n$

For this case, $\sqrt{P^2-\omega_n^2}$ is imaginary and the complementary solution may be written as

$$\overline{U}^C_{\mathrm{c}}(\zeta) = \mathrm{e}^{-P\zeta}\Big[B_1 \cos\Big(\sqrt{\omega_n^2-P^2}\zeta\Big) + B_2 \sin\Big(\sqrt{\omega_n^2-P^2}\zeta\Big)\Big], \tag{2.31}$$

the particular solution is written as

$$\overline{U}^C_{\mathrm{p}}(\zeta) = E_n \cos\frac{\zeta}{\mu} + F_n \sin\frac{\zeta}{\mu}, \tag{2.32}$$

and the general solution as

$$\overline{U}^C_n(\zeta) = \overline{U}^C_{\mathrm{c}}(\zeta) + \overline{U}^C_{\mathrm{p}}(\zeta). \tag{2.33}$$

For the given set of initial conditions,

$$B_1 = -E_n, \quad B_2 = \left(\frac{\gamma_+\gamma_- - 1}{2\beta_{\mathrm{c}}}\right)E_n,$$

$$E_n = \frac{4v^2}{\mu}\frac{1+\beta_c^2}{\big(1+\gamma_+^2\big)\big(1+\gamma_-^2\big)}, \quad F_n = \left(\frac{2v^2}{\mu}\right)^2 \frac{3-\gamma_+\gamma_-}{\big(1+\gamma_+^2\big)\big(1+\gamma_-^2\big)}, \tag{2.34}$$

with

$$\gamma_\pm = \beta_{\mathrm{c}} \pm \frac{1}{\mu P}, \quad \beta_{\mathrm{c}} = \sqrt{4v^2\lambda_n^2 - 1}. \tag{2.35}$$

Inserting the solutions obtained for the transformed variable into the inversion formula over the spectrum of all eigenvalues, and noticing that

$$N(\lambda_n) = \begin{cases} 1 & \text{for } n = 0, \\ \frac{1}{2} & \text{for } n \neq 0, \end{cases} \tag{2.36}$$

one obtains the mathematical expression for the temperature distribution through the region under consideration in the form

$$U(\eta,\zeta)=\overline{U}_0(\zeta)+2\sum_{n=1}^{M}\overline{U}_n^R(\zeta)\cos(\lambda_n\eta)+2\sum_{n=M+1}^{\infty}\overline{U}_n^C(\zeta)\cos(\lambda_n\eta), \tag{2.37}$$

where M is the number of real roots and $\overline{U}_0(\zeta)$, $\overline{U}_n^R(\zeta)$, and $\overline{U}_n^C(\zeta)$ are determined from Eqs. (2.25), (2.28) and (2.33), respectively.

3. Model validation

The mathematical analysis presented in Section 2 leads to a general analytic solution of the hyperbolic heat conduction problem in a finite medium subjected to a periodic heat source located at $\eta=0$. This result is validated analytically by considering the limiting case when $v=0$, for which case the temperature distribution predicted by the hyperbolic formulation should reduce to that predicted by the parabolic formulation.

3.1. Reduction to Fourier heat conduction

When v equals zero, the hyperbolic partial differential Eq. (2.5) reduces to the parabolic equation

$$\frac{\partial^2 U}{\partial\eta^2}=\frac{\partial U}{\partial\zeta}. \tag{3.1}$$

As $v\to 0$, $P\to\infty$ and $E_n=F_n=0$. Eq. (2.33) then reduces to $\overline{U}_n^C(\zeta)=0$. For this limiting case $\beta=\sqrt{P^2-\omega_n^2}\cong P-(\omega_n^2/2P)$ leading to the following

$$\exp\Big(-P+\sqrt{P^2-\omega_n^2}\Big)\zeta\to \mathrm{e}^{-\lambda_n^2},\quad \exp\Big(-P-\sqrt{P^2-\omega_n^2}\Big)\zeta\to 0,$$
$$A_1\to\frac{-\mu\lambda_n^2}{1+\mu^2\lambda_n^4},\quad C_n\to\frac{1}{1+\mu^2\lambda_n^4},\quad D_n\to\frac{\mu\lambda_n^2}{1+\mu^2\lambda_n^4}. \tag{3.2}$$

Inserting these results into Eq. (2.28), yields

$$\overline{U}_n^R(\zeta)=\frac{1}{1+\mu^2\lambda_n^4}\left[\sin\frac{\zeta}{\mu}+\mu\lambda_n^2\left(\cos\frac{\zeta}{\mu}-\mathrm{e}^{-\lambda_n^2\zeta}\right)\right], \tag{3.3}$$

and, consequently, Eq. (2.37) reduces to

$$U(\eta,\zeta)=\sin\frac{\zeta}{\mu}+2\sum_{n=1}^{\infty}\frac{\cos(\lambda_n\eta)}{1+\mu^2\lambda_n^4}\left[\sin\frac{\zeta}{\mu}+\mu\lambda_n^2\left(\cos\frac{\zeta}{\mu}-\mathrm{e}^{-\lambda_n^2\zeta}\right)\right]. \tag{3.4}$$

This is the same solution given by Eq. (A.5) in Appendix A, which is derived using the finite integral transform for the Fourier heat conduction described by the parabolic Eq. (3.1). Eq. (3.4) satisfies the initial conditions as well as the boundary condition given by the second of Eq. (2.6), it also satisfies the boundary condition given by the first of Eq. (2.6) in the sense of generalized functions [37].

Finally, the expression in Eq. (2.37) is equivalent to the analytic expression obtained in Ref. [33] using the Laplace transform method. However, the expression given by Eq. (2.37) is obtained in a straight forward manner, more compact and in a form which reflects the significance of the physical parameters involved, as will be shown in Section 4.

4. Results and discussion

The finite integral transform approach presented in this work eliminates the spatial variable and reduces the problem into an ODE in the temporal variable. The resulting equation is in the standard form used in studying mechanical and electrical oscillations (see for example Ref. [38]). One can, therefore, extend the well-known results obtained elsewhere onto the heat conduction problem described by a hyperbolic partial differential equation. From Eq. (2.21), one may recognize $2P\,\mathrm{d}\overline{U}/\mathrm{d}\zeta$ as a damping term with P as a damping parameter, ω_n as a characteristic angular frequency in the absence of damping and $\varpi = 1/\mu$ as the angular frequency of the driving force (the heat flux) defined in the right-hand side of Eq. (2.21).

As we noted in Section 2, in the solution $\overline{U}_n(\zeta) = \overline{U}_\mathrm{c}(\zeta) + \overline{U}_\mathrm{p}(\zeta)$, the complementary solution $\overline{U}_\mathrm{c}(\zeta)$ represents the transient effects and the terms contained in this solution damp out with time because of the factor $\exp(-P\zeta)$. The term $\overline{U}_\mathrm{p}(\zeta)$ represents the steady-state effects and contains the information for large values of time compared with v^2.

4.1. Application

We now study the details of the temperature distribution during the period before the transient effects have disappeared. We therefore consider a flat plate conductor, of dimensionless thickness equal unity, insulated at both sides and exposed to an oscillating heat flux with period ϖ and a dimensionless relaxation time (Vernotte number) v. Different values of ϖ and v were chosen to reflect different effects. Numerical computation was performed by utilizing the analytic solution obtained in Section 2.

For small values of the Vernotte number v, the damping effect becomes sufficiently large and the temperature is prevented from undergoing oscillation. For this case $P > \omega_n$ and the temperature may be considered as being *overdamped*. The temperature distribution due to the complementary solution approaches the equilibrium value asymptotically as shown in Fig. 2.

As v increases, the damping effects decreases resulting in increasing the temperature oscillation of the complementary solution. When P becomes less than ω_n, $(P < \omega_n)$, the temperature may be regarded as being *underdamped*. Eq. (2.31) can be written in the amplitude-phase form

$$\overline{U}_\mathrm{c}^C(\zeta) = D\mathrm{e}^{-P\zeta}\cos[\omega_1\zeta - \delta], \tag{4.1}$$

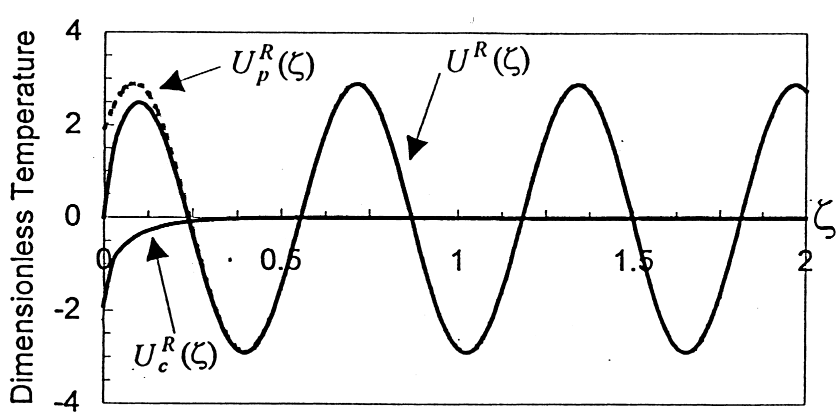

Fig. 2. The complementary and solutions and their sum for the overdamped temperature oscillation at the front surface ($v = 0.15, \varpi = 10$).

where D is the amplitude of the temperature oscillation, δ is a phase angle and $\omega_1 = \sqrt{\omega_n^2 - P^2}$. Because of the damping term $e^{-P\zeta}$ in Eq. (4.1), the temperature decays as it oscillates and the distribution is not periodic and, therefore, a frequency cannot be defined. The amplitude of the temperature oscillation in this case decreases with time. The envelope of the temperature versus time, is given by

$$U_{\mathrm{env}}(\eta,\zeta) = \pm 2\,e^{-P\zeta}\sum_{n=1}^{\infty} D\cos(\lambda_n\eta), \tag{4.2}$$

where $D = \sqrt{B_1^2 + B_2^2}$. Fig. 3 displays the temperature envelope, the transient (complementary) solution and the undamped (particular) solution at the front surface. The distribution of $U_{\mathrm{c}}^C(\eta,\zeta)$, $U_{\mathrm{p}}^C(\eta,\zeta)$ and their sum $U^C(\eta,\zeta)$ are displayed in Figs. 4 and 5 for different values of the driving frequency ϖ. When $\varpi < \omega_1$, the transient response of the temperature oscillation noticeably distorts the sinusoidal shape of the forcing function during the time interval immediately after the application of the driving force, Fig. 4. When $\varpi > \omega_1$, the effect is a modulation of the forcing function with little distortion of the high-frequency sinusoidal oscillation, Fig. 5. Both figures show the strong dependence of the transient distribution of the relative magnitudes of the frequency of the driving force and the damping frequency.

Numerical values of the analytic solution, Eq. (2.37), are evaluated at both the front and rear surfaces for $\varpi = 4$ and Vernotte number $v = 0.8$ and the result is displayed in Fig. 6. The jump points on the graph denote the moments at which the thermal wave front reaches the front and rear surfaces after propagation through the medium and a series of reflections at the two surfaces. Since the thickness (normalized) of the slab is 1.0 and the speed of propagation is $1/v$, the wave front takes a time equal to v from one side of the slab to the other. Thus, the jump points occur at times $2v$, $4v$, $6v, \ldots$ at the front surface and at times v, $3v$, $5v, \ldots$ at the rear surface. As time progresses, the jump points get lower and then disappear and the temperature response becomes a smooth periodic wave.

In searching for a limiting criterion of the transition from the parabolic to the hyperbolic heat conduction, the parabolic temperature response depicted by Eq. (3.4) and the hyperbolic temperature response depicted by Eq. (2.37) are evaluated for different values of v. The results are displayed in Fig. 7 for the front and the rear surfaces. It is noticed that the difference in the

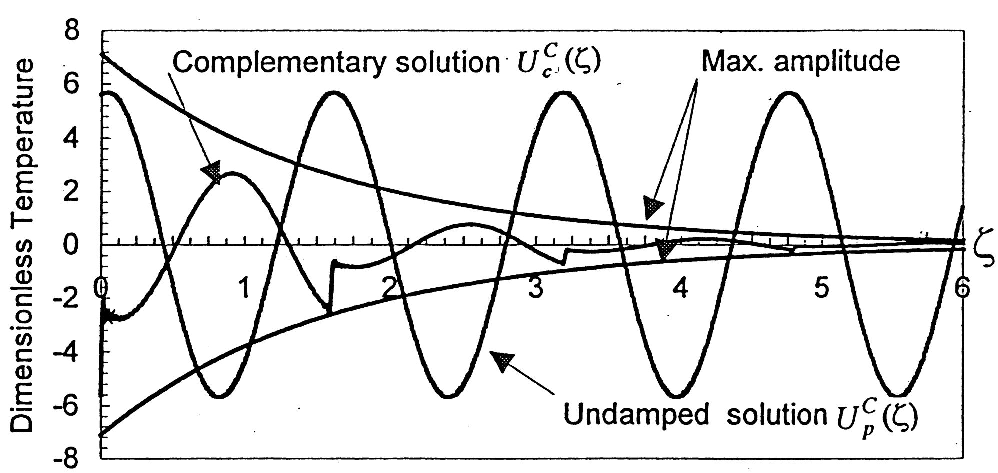

Fig. 3. The temperature envelope, the complementary (transient) and the particular (steady) solutions for the underdamped temperature oscillation at the front surface ($v = 0.8, \varpi = 4$).

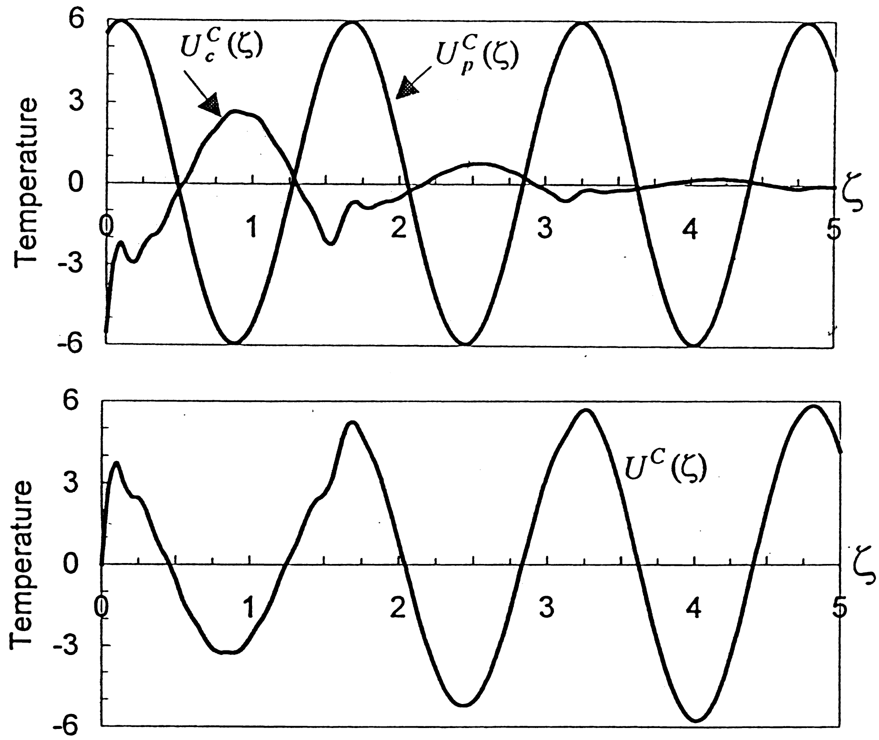

Fig. 4. The effect of the driving frequency on the complementary and particular solutions of the underdamped case at the front surface when $\varpi < \omega_1$.

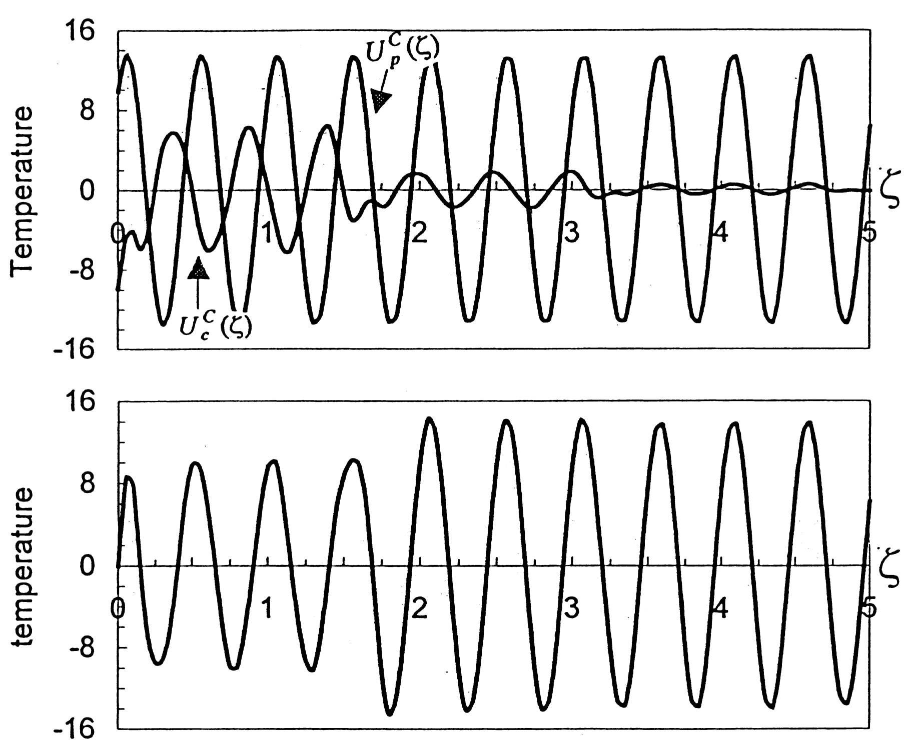

Fig. 5. The effect of the driving frequency on the complementary and particular solutions of the underdamped case at the front surface when $\varpi > \omega_1$.

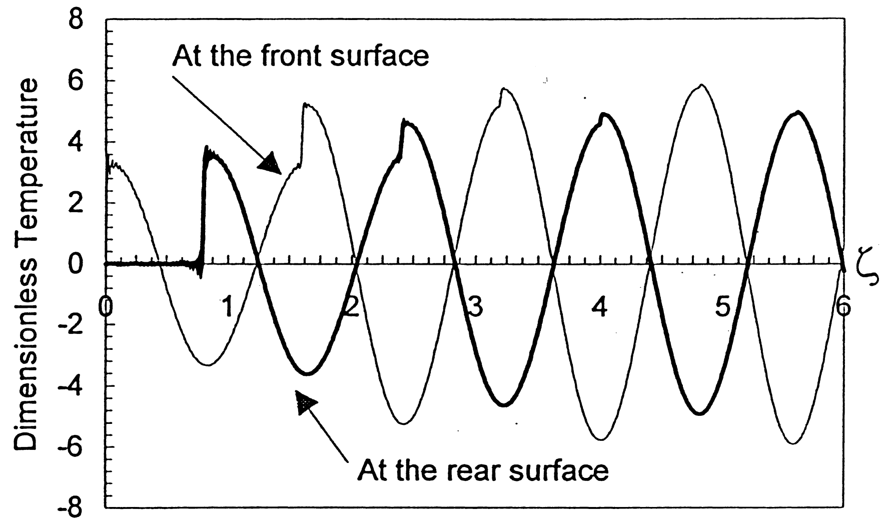

Fig. 6. The temperature distribution at the front and rear surfaces ($v = 0.8, \varpi = 4$).

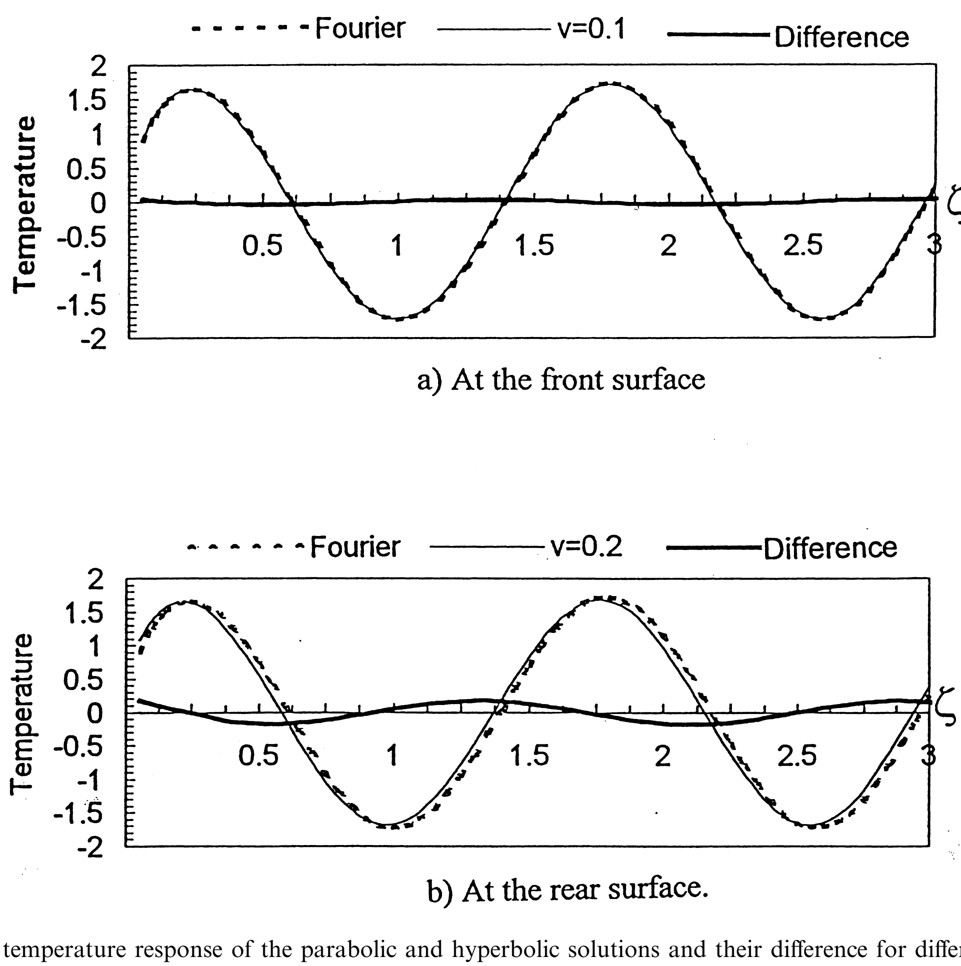

Fig. 7. The temperature response of the parabolic and hyperbolic solutions and their difference for different Vernotte numbers when $\varpi = 4$.

temperature distribution obtained from the parabolic and hyperbolic equations becomes insignificant whenever $v \leqslant 0.1$. That is, $v > 0.1$ is the limiting criterion for the occurrence of differences in temperature response between the parabolic and hyperbolic modelling of heat conduction.

4.2. Amplitude and phase

The analytic solution given by Eq. (2.37) is rewritten in the following detailed form

$$U(\eta,\zeta) = \sin(\omega\zeta) + 2\sum_{n=1}^{M}\left(\overline{U}_{\mathrm{c}}^{R} + \overline{U}_{\mathrm{p}}^{R}\right)\cos(\lambda_n\eta) + 2\sum_{n=M+1}^{\infty}\left(\overline{U}_{\mathrm{c}}^{C} + \overline{U}_{\mathrm{p}}^{C}\right)\cos(\lambda_n\eta), \tag{4.3}$$

As indicated above, $\overline{U}_{\mathrm{c}}^{R}$ decays asymptotically and $\overline{U}_{\mathrm{c}}^{C}$ is not periodic because of the $\mathrm{e}^{-P\zeta}$ term. The effect of both parts dies out with time and the temperature distribution eventually will be given by the remaining terms of Eq. (4.3) which are all periodic. Upon the utilization of Eqs. (2.27) and (2.32), the temperature distribution becomes

$$U(\eta,\zeta) = \Gamma\sin(\varpi\zeta) + \Pi\cos(\varpi\zeta). \tag{4.4}$$

This equation can be written in the amplitude-phase form

$$U(\eta,\zeta) = A\cos(\varpi\zeta - \phi), \tag{4.5}$$

where the amplitude A is given by

$$A = \sqrt{\Gamma^2 + \Pi^2}, \tag{4.6}$$

and the phase angle ϕ is given by

$$\phi = \tan^{-1}\left(\frac{\Gamma}{\Pi}\right), \tag{4.7}$$

where

$$\Gamma = 1 + 2\sum_{n=1}^{M} C_n\cos(\lambda_n\eta) + 2\sum_{n=M+1}^{\infty} F_n\cos(\lambda_n\eta),$$

$$\Pi = 2\sum_{n=1}^{M} D_n\cos(\lambda_n\eta) + 2\sum_{n=M+1}^{\infty} E_n\cos(\lambda_n\eta). \tag{4.8}$$

The quantity ϕ represents the phase difference between the driving force and the resultant temperature; a real delay occurs between the action of the driving force and the temperature response.

Eq. (4.6) is used to evaluate the amplitude difference between the front and the rear surfaces for different values of Vernotte number and the result is shown in Fig. 8(a). This curve agrees with the numerical results in Ref. [33]. The phase difference between the front and the rear surfaces is evaluated from Eq. (4.7) and the result is shown in Fig. 8(b).

As $v \to 0$, both figures indicate that the amplitude difference and the phase difference of the hyperbolic formulation approach those of the parabolic one. With the increase of v (enhancement of the non-Fourier effects), the amplitude damping and the phase difference deviate relatively from their parabolic correspondent. The deviation of the phase difference indicates that the hyperbolic formulation predicts a relative low speed of thermal disturbance propagation, while the

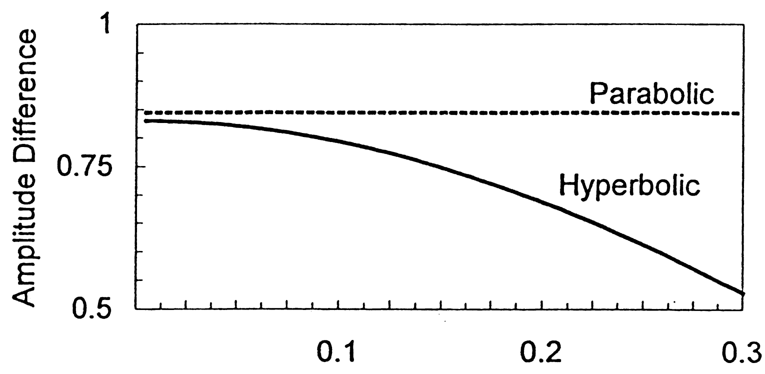

a

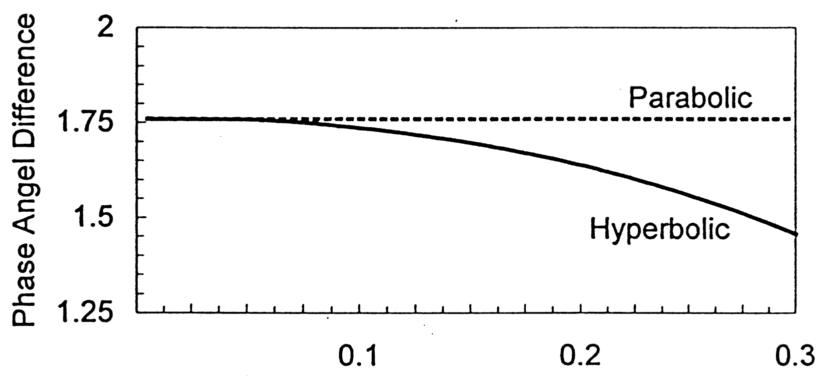

b

Fig. 8. (a) The amplitude difference of temperature oscillation at the front and the rear surfaces for different Vernotte numbers. (b) The phase angle difference of temperature oscillation at the front and the rear surfaces for different Vernotte numbers.

deviation of the amplitude difference indicates that the damping in amplitude decreases with the increase of the non-Fourier effects.

5. Conclusion

An analytic solution of the non-Fourier heat conduction in a finite medium insulated at both sides and subjected to a periodic heat flux is obtained by the use of the finite integral transform technique. For the limiting case as the relaxation time equals zero, the obtained temperature response from the non-Fourier (hyperbolic) formulation reduces to the temperature response obtained from the classical Fourier (parabolic) formulation. Solutions to hyperbolic heat conduction problems are non-Fourier thermal waves damped by heat diffusion. In contrast, Fourier solutions show conduction only by diffusion. Further, solutions to hyperbolic problems converge to corresponding Fourier solutions for sufficiently large time after thermal disturbances (i.e. imposition of heat fluxes) because of wave damping.

A transition criterion from the hyperbolic formulation to the parabolic formulation is found to appear when $v > 0.1$. A simple analytical expression of the phase and amplitude of thermal oscillation is given. It is shown that the hyperbolic formulation predicts a relatively low speed of thermal disturbance propagation and that the damping in amplitude decreases with the increase of the non-Fourier effects. The mathematical treatment in this work leads to an analytic solution of the hyperbolic heat conduction problem in a straight forward and systematic way.

Appendix A. Finite integral transform solution of Fourier heat conduction in a finite medium exposed to periodic heat flux

For this situation, the boundary and initial conditions associated with Eq. (3.1) are

$$\frac{\partial}{\partial \eta} U(0,\zeta) = -\frac{1}{\mu}\cos\frac{\zeta}{\mu}, \quad \frac{\partial}{\partial \eta} U(1,\zeta) = 0 \quad \text{and} \quad U(\eta,0) = 0 \tag{A.1}$$

The eigenvalue problem associated with the homogeneous part of the current problem is given by

$$\Phi'' + \lambda_n^2 \Phi = 0 \quad \text{with } \Phi'(0) = \Phi'(1) = 0. \tag{A.2}$$

Operating on Eq. (3.1) by $\int_0^1 \Phi(\eta)\,\mathrm{d}\eta$, integrate the left side by parts twice, then operate on Eq. (A.2) with $\int_0^1 u(\eta,\zeta)\,\mathrm{d}\eta$, utilize the definition of the integral transform, substitute for the surface conditions and simplify to get

$$\frac{\mathrm{d}\overline{U}_n}{\mathrm{d}\zeta^2} + \lambda_n^2 \overline{U}_n = \frac{1}{\mu}\cos\frac{\zeta}{\mu} \tag{A.3}$$

subject to the transformed initial condition $\overline{U}_n(0) = 0$. The solution of this system is evaluated to

$$\overline{U}_n(\zeta) = \frac{1}{1+\mu^2\lambda_n^4}\left[\sin\frac{\zeta}{\mu} + \mu\lambda_n^2\left(\cos\frac{\zeta}{\mu} - \mathrm{e}^{-\lambda_n^2\zeta}\right)\right]. \tag{A.4}$$

Now substituting in the inversion formula over all the spectra of eigenvalues to obtain the temperature distribution of the parabolic heat conduction in the form

$$U(\eta,\zeta) = \sin\frac{\zeta}{\mu} + 2\sum_{n=1}^{\infty}\frac{\cos(\lambda_n\eta)}{1+\mu^2\lambda_n^4}\left[\sin\frac{\zeta}{\mu} + \mu\lambda_n^2\left(\cos\frac{\zeta}{\mu} - \mathrm{e}^{-\lambda_n^2\zeta}\right)\right] \tag{A.5}$$

References

[1] H. Jackson, C.I. Walker, Thermal conductivity, second sound and phonon–phonon interactions in NaF, Phys. Rev. B 3 (1971) 1428–1439.
[2] V. Narayanamurti, R.C. Dynes, Observation of second sound in bismuth, Phys. Rev. Lett. 28 (1972) 1561–1565.
[3] B. Bertmann, D.J. Sandiford, Second sound in solid helium, Sci. Am. 222 (5) (1970) 92–101.
[4] W. Kaminski, Hyperbolic heat conduction for materials with a non-homogeneous inner structure, ASME J. of Heat Transfer 112 (1990) 555–560.
[5] D.J. Wall, P. Olsson, Invariant imbedding and hyperbolic heat waves, J. Math. Phys. 38 (3) (1997) 1723–1749.
[6] K. Mitra, S. Kumar, A. Vedavarz, M.K. Moallemi, Experimental evidence of hyperbolic heat conduction in processed meat, J. Heat Transfer 117 (1995) 568–773.
[7] H. D Weymann, Finite speed of propagation in heat conduction, diffusion and viscous shear motion, Am. J. Phys. 35 (1967) 488–496.
[8] M.E. Gurtin, A.C. Pipkin, A general theory of heat conduction with finite wave speed, Aechs. ration. Mech. Analysis 31 (1968) 113–126.
[9] M.J. Maurer, Relaxation model for heat conduction in metals, J. Appl. Phys. 40 (1972) 5123–5130.
[10] V. Taitel, On the parabolic, hyperbolic and discrete formulation of heat conduction equation, Int. J. Heat Mass Transfer 15 (1972) 369–371.
[11] A.V. Luikov, V.A. Bubnov, I.A. Soloview, On the wave solutions of heat conduction equation, Int. J. Heat Mass Transfer 19 (1976) 245–248.
[12] J.I. Frankel, B. Vick, M.N. Ozisik, Flux formulation of hyperbolic heat conduction, J. Appl. Phys. 58 (9) (1985) 3340–3345.

[13] A. Barletta, E. Zanchini, Hyperbolic heat conduction and local equilibrium: a second law analysis, Int. J. Heat Mass Transfer 40 (1997) 1007–1016.
[14] A.E. Kronberg, A.H. Benneker, K.R. Westerterp, Notes on wave theory in heat conduction: A new boundary condition, Int. J. Heat Mass Transfer 41 (1) (1998) 127–137.
[15] P. Vernotte, Les panadoxes de la theorie continue de l'equatioin de la chaleur, C.R. Acad. Sci. 246 (1958) 3154–3155.
[16] C. Cattaneo, Sur une forme de l'equation de la chaleur elinant le paradoxes d'une propagation instantance, C.R. Acad. Sci. 247 (1958) 431–432.
[17] D.Y. Tzou, Thermal shock waves induced by a moving crack, J. Heat Transfer 112 (1990) 21–27.
[18] A.M. Mullis, Rapid solidification within the framework of a hyperbolic conduction model, Int. J. Heat Mass Transfer 40 (17) (1997) 4085–4094.
[19] P.J. Antaki, Analysis of hyperbolic heat conduction in a semi-infinite slab with surface convection, Int. J. Heat mass Transfer 40 (13) (1997) 3247–3250.
[20] B.B. Mikic, A model rate equation for transient thermal conduction, Int. J. Heat Mass Transfer 10 (1967) 1899–1904.
[21] K.J. Baumeister, T.D. Hamill, Hyperbolic heat conduction equation- a solution for the semi-infinite body problem, J. Heat Transfer 91 (1969) 543–548.
[22] K.J. Baumeister, T.D. Hamill, Hyperbolic heat conduction equation- a solution for the semi-infinite body problem, J. Heat Transfer 93 (1971) 126–127.
[23] M.J. Maurer, H.A. Thompson, Non-Fourier effects at high heat flux, J. Heat Transfer 95 (1983) 284–286.
[24] B. Vick, M.N. Ozisik, Growth and decay of a thermal pulse predicted by the hyperbolic heat conduction equation, J. Heat Transfer 105 (1983) 902–907.
[25] A. Barleta, E. Zarchini, Hyperbolic heat conduction and thermal resonances in a cylindrical solid carrying a steady-periodic electric field, Int. J. Heat Mass Transfer 39 (1996) 1307–1315.
[26] G.F. Carey, M. Tsai, Hyperbolic heat transfer with reflection, Numer. Heat Transfer 5 (1982) 309–327.
[27] M.N. Ozisik, B. Vick, Propagation and reflection of thermal waves in a finite medium, Int. J. Heat Mass Transfer 27 (1984) 1845–1854.
[28] D.E. Glass, M.N. Ozisik, B. Vick, Hyperbolic heat conduction with surface radiation, Int. J. Heat Mass Transfer 28 (1985) 1823–1830.
[29] D.E. Glass, M.N. Ozisik, D.S. McRae, B. Vick, Hyperbolic heat conduction with temperature-dependent thermal conductivity, J. Appl. Phys. 59 (1986) 1861–1865.
[30] J. Gembarovic, V. Majernik, Non-Fourier propagation of heat pulse in finite medium, Int. J. Heat Mass Transfer 31 (1988) 1073–1081.
[31] Z.M. Tan, W.J. Yang, Heat transfer during asymmetrical collision of thermal waves in a thin film, Int. J. Heat Mass Transfer 41 (17) (1997) 3999–4006.
[32] D.W. Tang, N. Araki, Non-Fourier heat conduction in a finite medium under periodic surface thermal disturbance, Int. J. Heat Mass Transfer 39 (8) (1996) 1585–1590.
[33] D.W. Tang, N. Araki, Non-Fourier heat conduction in a finite medium under periodic surface thermal disturbance-II. Another form of solution, Int. J. Heat Mass Transfer 39 (15) (1996) 3305–3308.
[34] B. Abdel-Hamid, Transient temperature distribution of periodic heat diffusion in a flat plate crossed by an alternating electric current, Appl. Math. Modelling 20 (1997) 387–393.
[35] B. Abdel-Hamid, Analysis of transient periodic heat transfer in a flat plate carrying an alternating electric current, in: Proceedings of the International Conference on Application of Mathematics and Engineering and Science, Morocco, 1996, pp. 143–147.
[36] P. O'Neil, Advanced Engineering Mathematics, PWS, 1995.
[37] M.J. Lighthill, An Introduction to Fourier Analysis and Generalized Functions, Cambridge University Press, Cambridge, 1980.
[38] J.B. Marion, S.T. Thornton, Classical Dynamics of Particles and Systems, Saunders, New York, 1995.